Research Square

Preprints are preliminary reports that have not undergone peer review.
They should not be considered conclusive, used to inform clinical practice,
or referenced by the media as validated information.

An Improved Adaptive Sliding Window Kalman Filter Approach for Target Tracking under Outlier Observations

Miaomiao Wang
Shanxi College Of Applied Science And Technology
Zhentao Wang
dzwztmail@163.com

Harbin Institute of Technology
Ziyan Ni
CNOOC (China) Ltd. Shenzhen Branch
Xue Wang
Sinopec Petroleum Engineering Design Co., Ltd
Lifei Liang
Shanxi College Of Applied Science And Technology

Research Article

Keywords: Adaptive, Kalman filtering, Variational Bayesian, Moving median, Outliers

Posted Date: September 16th, 2026

DOI: https://doi.org/10.21203/rs.3.rs-8053572/v1

License: This work is licensed under a Creative Commons Attribution 4.0 International License.
Read Full License

Additional Declarations: No competing interests reported.

An Improved Adaptive Sliding Window Kalman Filter Approach for Target Tracking under Outlier Observations

MiaomiaoWang[1)], Zhentao Wang [2†)], Ziyan Ni[3)] ,Xue Wang[4)], Lifei Liang[5)]

1) (Shanxi College Of Applied Science And Technology, *Taiyuan, 030062, China, wmiaomiao0418@163.com*)

2) (Harbin Institute of Technology, Harbin, 150006, China, dzwztmail@163.com)

3) (CNOOC (China) Ltd. Shenzhen Branch, Shenzhen, 518000, Chinanizy@cnooc.com.cn)

4) Sinopec Petroleum Engineering Design Co., Ltd.,Dongying,257000,China,wangxue20220423@163.com

5) (Shanxi College Of Applied *S*cience *A*nd *T*echnology, *Taiyuan, 030062, China, qiqi519@163.com*)

†Correspondence: dzwztmail@163.com (Zhentao Wang)

Abstract

To address the limited estimation accuracy of traditional Kalman filters in environments with unknown noise, this study proposes an modified Modified Median Adaptive Probabilistic Relaxed Iterative Variational Bayesian Kalman Filter (MMAPRIVBKF) method. This approach enables the adaptive learning of the unknown target state covariance matrix and measurement noise covariance matrix. Through the synergistic interaction of Forward Kalman filtering (KF), Backward Kalman Smoothing (KS), and noise covariance matrix estimation, real-time online estimation of the system state is achieved. By approximating the smoothed posterior distribution of the state vectors within the slide window and integrating variational Bayesian methods, the algorithm updates the posterior distribution of the noise covariance matrix to an inverse Wishart distribution. This approach effectively avoids the fixed-point iteration inherent in traditional methods, thereby ensuring high computational efficiency. Furthermore, to address the potential random disturbances or outliers within the slide window, an innovative slide median window was adopted. This maintains noise adaptability while further enhancing the state-estimation accuracy. Simulation experiments demonstrated that compared with the original slide window variational adaptive Kalman filtering method, the proposed approach reduced the root mean square error (RMSE) for distance, bearing, and velocity by 11.11%, 1.78%, and 3.16%, respectively, fully validating the superiority and practical value of the algorithm.

INDEX TERMS Adaptive · Kalman filtering · Variational Bayesian · Moving median · Outliers

1 INTRODUCTION

Since the introduction of the Kalman Filter (KF) theory, its optimal estimation properties in linear Gaussian systems have established it as a core algorithm in various engineering fields, including target tracking, navigation and positioning, and signal processing [1]–[3]. The classical Kalman filter is based on discrete-time linear state-space models and performs state estimation through a recursive "time update-measurement update" process. However, its performance heavily relies on the precise prior knowledge of the state noise covariance matrix (SNCM) and measurement noise covariance matrix (MNCM) [4-8]. In real-world systems, the statistical properties of noise are often unknown or time-varying. Any deviation between the pre-set noise covariance and actual values can lead to significant degradation in filtering accuracy or even cause filtering divergence [9].

As engineering applications increasingly advance into complex nonlinear scenarios, the linear assumption of classical Kalman filtering struggles to meet practical demands, which drives the development of nonlinear Kalman filtering methods. Methods such as the Unscented Kalman Filter (UKF) and Cubature Kalman Filter (CKF) approximate the probability distribution of nonlinear functions, avoid direct linearization, and exhibit superior estimation performance in nonlinear systems [10-11]. However, these methods are heavily reliant on prior knowledge of the noise covariance matrix. When the statistical properties of the system noise are unknown or exhibit time-varying characteristics, the estimation accuracy and robustness remain constrained.

To address the uncertainty in noise statistics, Adaptive Kalman Filtering (AKF) has emerged as a research hotspot. Early adaptive approaches primarily adjusted filtering gains in real time by online estimation of the noise covariance matrix. Examples include recursive estimation methods based on residual sequences and multi-model adaptive filtering [12-15], which partially enhance adaptability to noise uncertainty. However, most existing adaptive Kalman filtering methods, particularly those based on Variational Bayesian (VB) approaches such as the VBAKF-PR scheme [16-17], suffer from a critical flaw: their

performance exhibits strong dependence on the predefined "nominal SNCM". Significant deviations between the nominal SNCM and its true value, or unreasonable initial settings for variational iterations, can slow convergence, degrade estimation accuracy, or even trigger numerical instability, making it difficult to adapt to real-world scenarios with rapidly changing noise statistics.

To reduce the dependence on nominal SNCM and enhance the dynamic adaptability in noise estimation, Huang et al. proposed a slide window-based adaptive Kalman filtering method [18]. This approach employs a sliding time window of length L to jointly infer the noise covariance matrix using the measurements and state estimates from multiple time points within the window. This mitigates the impact of single-point data perturbations and improves the tracking capability for time-varying noise. However, the logic of this method often centers on "a single analysis", performing a Kolmogorov-Smirnov (KS) test only once on the "final fixed dataset" or "single iteration output of the model," ultimately yielding a single statistic as the core basis for the judgment. A single test result is susceptible to "random data fluctuations" or "local outlier samples". If the dataset for a single analysis contains sampling bias or if the single iteration result is affected by accidental interference, the single statistic may fail to accurately reflect the overall characteristics of the data or model, leading to biased inferential conclusions.

To address these issues, this study proposes an adaptive Kalman filtering method based on slide window medians. While preserving the adaptability of the slide window to time-varying noise and its low nominal SNCM dependency characteristics, this approach effectively enhances the real-time performance of the algorithm. This approach introduces a "slide window median" mechanism within the slide window framework, achieving dual optimization. First, it employs a variational Bayesian method for analytical updates of the noise covariance matrix, approximating the posterior distribution as an inverse Wishart distribution. This avoids fixed-point iterations, thereby ensuring estimation efficiency and accuracy. Second, it leverages the inherent robustness of the median against outliers and data compression capabilities to mitigate the impact of random disturbances on the filtering process, ultimately providing more robust and reliable results for system state estimation.

2 Method

An appropriate probabilistic model must be established to compute the joint posterior probability distribution $p\left(x_{k-L:k}, Q^{(k)}, R^{(k)} | z_{1:k}\right)$ online. Considering that the SNCM and MNCM typically change slowly in practical systems, this study assumes that within the slide window interval $j \in [k-L, k]$, the SNCM and MNCM at all time points can be approximated as $Q^{(k)}$ and $R^{(k)}$, respectively, corresponding to the current time point k. Based on this assumption, the state transition Probability Density Function (PDF) $p\left(\mathbf{x}_j | \mathbf{x}_{j-1}, \mathbf{Q}^{(k)}\right)$ and measurement likelihood PDF $p\left(\mathbf{z}_j | \mathbf{x}_j, \mathbf{R}^{(k)}\right)$ at each time point within the window can be expressed as follows:

$$\begin{cases} p\left(\mathbf{x}_j | \mathbf{x}_{j-1}, \mathbf{Q}^{(k)}\right) = \mathrm{N}\left(\mathbf{x}_j; \mathbf{F}_j \mathbf{x}_{j-1}, \mathbf{Q}^{(k)}\right) \\ p\left(\mathbf{z}_j | \mathbf{x}_j, \mathbf{R}^{(k)}\right) = \mathrm{N}\left(\mathbf{z}_j; \mathbf{H}_j \mathbf{x}_j, \mathbf{R}^{(k)}\right) \end{cases} \quad (1)$$

Where: $\mathbf{F}_j$ and $\mathbf{H}_j$ denote the state transition and measurement matrices, respectively.

When the mean of a Gaussian distribution is known, the conjugate prior PDF of the covariance matrix is typically the inverse Wishart distribution [19-20]. To facilitate conjugate Bayesian inference, this study models the prior distributions $p\left(Q^{(k)} | z_{1:k-1}\right)$ of the covariance matrices $Q^{(k)}$ and $R^{(k)}$ as inverse Wishart distribution, that is,

$$\begin{cases} p\left(\mathbf{Q}^{(k)} | \mathbf{z}_{1:k-1}\right) = \mathrm{IW}\left(\mathbf{Q}^{(k)}; \hat{y}_{k|k-1}, \bar{\mathbf{Y}}_{k|k-1}\right) \\ p\left(\mathbf{R}^{(k)} | \mathbf{z}_{1:k-1}\right) = \mathrm{IW}\left(\mathbf{R}^{(k)}; \hat{u}_{k|k-1}, \bar{\mathbf{U}}_{k|k-1}\right) \end{cases} \quad (2)$$

Where: $\hat{y}_{k|k-1}$ and $\hat{u}_{k|k-1}$ are the degrees of freedom parameters, and a $\bar{\mathbf{Y}}_{k|k-1}$ nd $\bar{\mathbf{U}}_{k|k-1}$ are the corresponding inverse scale matrices.

In engineering practice, it is often challenging to establish explicit evolutionary models for Noise Covariance Matrices (NCMs) [21]. However, the actual system noise typically exhibits slow temporal variation characteristics. Based on this, it can be assumed that the prior PDF of $Q^{(k)}$ at the current time $R^{(k)}$ share the same mean as the previous PDF at the last time step. However, owing to the unclear evolution mechanism, their uncertainty should slightly increase. To address this, this study adopts the approach from [22] by introducing a decay factor ρ to propagate the approximate posterior distribution of the NCMs. The prior parameters were constructed as follows:

$$\begin{cases} \hat{y}_{k|k-1} = \rho \hat{y}_{k-1|k-1}, & \bar{\mathbf{Y}}_{k|k-1} = \rho \bar{\mathbf{Y}}_{k-1|k-1} \\ \hat{u}_{k|k-1} = \rho \hat{u}_{k-1|k-1}, & \bar{\mathbf{U}}_{k|k-1} = \rho \bar{\mathbf{U}}_{k-1|k-1} \end{cases} \quad (3)$$

ρ is the forgetting factor used to characterize the slow temporal evolution of the SNCM and MNCM. To ensure the estimation accuracy and numerical stability of the filter, it is recommended to set ρ between 0.9 and 1.0. Subsequently, based on the model established in Equations (1)–(3), the joint posterior probability $p\left(\mathbf{x}_{k-L:k}, \mathbf{Q}^{(k)}, \mathbf{R}^{(k)} \middle| \mathbf{z}_{1:k}\right)$ was inferred using the VB method.

Following the standard VB approach, assuming independence between the state vector and NCMs, the joint posterior distribution $p\left(\mathbf{x}_{k-L:k}, \mathbf{Q}^{(k)}, \mathbf{R}^{(k)} | \mathbf{z}_{1:k}\right)$ can be approximated as the following factorized form [23]:

$$p\left(\mathbf{x}_{k-L:k}, \mathbf{Q}^{(k)}, \mathbf{R}^{(k)} \middle| \mathbf{z}_{1:k}\right) \approx q\left(\mathbf{x}_{k-L:k}\right) q\left(\mathbf{Q}^{(k)}\right) q\left(\mathbf{R}^{(k)}\right) \quad (4)$$

Where each approximate posterior density function $q(\theta)$ satisfies the following unified expression:

$$\begin{cases} \log q(\theta) = \mathrm{E}_{\Xi^{-\theta}}\left[\log p(\Xi, \mathbf{z}_{1:k})\right] + c_\theta \\ \Xi \supseteq \{\mathbf{x}_{k-L:k}, \mathbf{Q}^{(k)}, \mathbf{R}^{(k)}\} \end{cases} \quad (5)$$

Where: Ξ denotes the set of all variables to be estimated, θ represents any variable in the set Ξ, $\Xi^{-\theta}$ denotes the set of variables in Ξ excluding θ,

and c_θ is a constant that is independent of θ.

Equations (4) and (5) reveal that the variational posterior parameters $\mathbf{x}_{k-L:k}$, $\mathbf{Q}^{(k)}$ and $\mathbf{R}^{(k)}$ exhibit mutual coupling [24]. Traditionally, fixed-point iteration methods are employed to approximate solutions; however, this approach incurs a high computational complexity. To circumvent iterative processes and enhance computational efficiency, this study proposes analytical updates for $q(\mathbf{Q}^{(k)})$ and $q(\mathbf{R}^{(k)})$, as detailed in Proposition 1 below.

Furthermore, leveraging the structure of Equation (3), we approximate $q(\mathbf{x}_{k-L:k})$ as follows:

$$q(\mathbf{x}_{k-L:k}) \approx \mathrm{N}\ (\mathbf{x}_{k-L:k}; \hat{\mathbf{x}}_{k-L:k|k}^{(k-1)}, \mathbf{P}_{k-L:k|k}^{(k-1)}) \quad (6)$$

Proposition 1: Based on the model established by Equation (6) and subsequent Equations (7)–(9), the posterior probability density functions of $\mathbf{Q}^{(k)}$ and $\mathbf{R}^{(k)}$ can be analytically updated to the following inverse Wishart distribution:

$$\begin{cases} q(\mathbf{Q}^{(k)}) = \mathrm{IW}(\mathbf{Q}^{(k)}; \hat{y}_{k|k}, \bar{\mathbf{Y}}_{k|k}) \\ q(\mathbf{R}^{(k)}) = \mathrm{IW}(\mathbf{R}^{(k)}; \hat{u}_{k|k}, \bar{\mathbf{U}}_{k|k}) \end{cases} \quad (7)$$

Where the parameters $\hat{y}_{k|k}$, $\bar{\mathbf{Y}}_{k|k}$, $\hat{u}_{k|k}$ and $\bar{\mathbf{U}}_{k|k}$ are given by

$$\begin{cases} \hat{y}_{k|k} = \hat{y}_{k|k-1} + L, & \bar{\mathbf{Y}}_{k|k} = \bar{\mathbf{Y}}_{k|k-1} + \sum_{j=k-L+1}^{k} \mathbf{A}_j \\ \hat{u}_{k|k} = \hat{u}_{k|k-1} + L + 1, & \bar{\mathbf{U}}_{k|k} = \bar{\mathbf{U}}_{k|k-1} + \sum_{j=k-L}^{k} \mathbf{B}_j \end{cases} \quad (8)$$

Auxiliary matrices $\mathbf{A}_j$ and $\mathbf{B}_j$ are defined as

$$\begin{cases} \mathbf{A}_j = \mathrm{E}\left[(\mathbf{x}_j - \mathbf{F}_j\mathbf{x}_{j-1})(\mathbf{x}_j - \mathbf{F}_j\mathbf{x}_{j-1})^T\right] \\ \mathbf{B}_j = \mathrm{E}\left[(\mathbf{z}_j - \mathbf{H}_j\mathbf{x}_j)(\mathbf{z}_j - \mathbf{H}_j\mathbf{x}_j)^T\right] \end{cases} \quad (9)$$

The proof of Proposition 1 is provided in [25]. Using Equations (6) and (9), the aforementioned mathematical expectation can be further calculated as follows:

$$\begin{aligned} \mathbf{A}_j &= \mathbf{P}_{j|k}^{(k-1)} - \mathbf{F}_j\mathbf{P}_{j-1,j|k}^{(k-1)} - \left[\mathbf{P}_{j-1,j|k}^{(k-1)}\right]^T\mathbf{F}_j^T + \mathbf{F}_j\mathbf{P}_{j-1|k}^{(k-1)}\mathbf{F}_j^T \\ &\quad + \left[\hat{\mathbf{x}}_{j|k}^{(k-1)} - \mathbf{F}_j\hat{\mathbf{x}}_{j-1|k}^{(k-1)}\right]\left[\hat{\mathbf{x}}_{j|k}^{(k-1)} - \mathbf{F}_j\hat{\mathbf{x}}_{j-1|k}^{(k-1)}\right]^T \end{aligned} \quad (10)$$

$$\begin{aligned} \mathbf{B}_j &= \left[\mathbf{z}_j - \mathbf{H}_j\hat{\mathbf{x}}_{j|k}^{(k-1)}\right]\left[\mathbf{z}_j - \mathbf{H}_j\hat{\mathbf{x}}_{j|k}^{(k-1)}\right]^T \\ &\quad + \mathbf{H}_j\mathbf{P}_{j|k}^{(k-1)}\mathbf{H}_j^T \end{aligned} \quad (11)$$

Where: $\hat{x}_{j|k}$ and $P_{j|k}$ denote the smooth estimates of the state at time step j and their error covariance matrices based on all window data, respectively. $\mathbf{P}_{j-1,j|k}$ represents the cross-covariance matrix between the smooth errors at time steps j-1 and j, whose expression is given in [26]:

$$\mathbf{P}_{j-1,j|k}^{(k-1)} = \mathbf{G}_{j-1}^{(k-1)}\mathbf{P}_{j|k}^{(k-1)} \quad (12)$$

Where: $\mathbf{G}_{j-1}$ denotes the smoothing gain matrix at time step j−1.

According to Proposition 1, the estimated values of $\mathbf{Q}^{(k)}$ and $\mathbf{R}^{(k)}$ can be calculated as follows.

$$\begin{cases} \bar{\mathbf{Q}}^{(k)} = \left\{\mathrm{E}\left[(\bar{\mathbf{Q}}^{(k)})^{-1}\right]\right\}^{-1} = \bar{\mathbf{Y}}_{k|k} / \hat{y}_{k|k} \\ \bar{\mathbf{R}}^{(k)} = \left\{\mathrm{E}\left[(\bar{\mathbf{R}}^{(k)})^{-1}\right]\right\}^{-1} = \bar{\mathbf{U}}_{k|k} / \hat{u}_{k|k} \end{cases} \quad (13)$$

The slide window variational adaptive Kalman filter (SWVAKF) proposedin this paper consists of three components: Forward KF, Backward KS, and an online estimation module for $\mathbf{Q}^{(k)}$ and $\mathbf{R}^{(k)}$ implemented based on Equations (7), (8), (10), and (13).

To reduce the computational overhead in traditional slide window adaptive Kalman filtering, this study proposes an improved strategy based on the slide median window. Unlike conventional slide window, this method fully leverages the statistical properties of the data stream by selecting the median as the benchmark for window updates in every iteration. This approach enhances the estimation accuracy while optimizing the computational efficiency.

Traditional slide window typically perform a single KS test on the final dataset or a single iteration result, outputting a single statistic as the basis for the judgment. However, a single result may be affected by random fluctuations or local anomalies, leading to inference bias [27]. In contrast, the iterative median strategy proposed in this study enhances result robustness by increasing representativeness through multiple iterations and reducing random error interference via the median [28]. Let the KS process parameters be stored as

$$A_k = [a_{k-L}, a_{k-L+1}, \cdots, a_k], B_k = [b_{k-L}, b_{k-L+1}, \cdots, b_k] \quad (14)$$

Where: L denotes window size. The median of the window is calculated as follows:

$$\mathrm{Med}_t = \mathrm{median}(A_t) \quad (15)$$

$$\mathrm{Med}_t = \mathrm{median}(B_t) \quad (16)$$

If the window size L is odd, the median is the value at position $(w+1)/2$ after sorting; if it is even, it is the value at position $(w/2+1)$ The resulting median is output as a value at the corresponding window position. The complete implementation flow of the proposed method is presented in Algorithm 1.

3 Simulation

In this section, the performance of the proposed MMAPRIVBKF algorithm is evaluated using simulation tests. Using a submerged target moving in a uniform linear motion as the target state, the advantages of the proposed filter were demonstrated using a two-dimensional target tracking model. The simulation results under various noise scenarios are compared with those of the traditional Extended Kalman Filter (EKF)[29] and NAPRIVBKF[18]. MATLAB 2022a simulations were conducted on a configuration including an AMD Ryzen 5 5600G processor (6 cores, base frequency 3.90 GHz) with 8 GB of memory.

3.1 Initial Parameter Settings

To validate the performance of the proposed MMAPRIVBKF algorithm, a two-dimensional target-tracking simulation scenario was constructed. In this scenario, the target motion state is described by vector. And represent the horizontal and vertical coordinates of the target, respectively. The state equation and measurement equation are shown in(17) and (18), respectively, where the coefficient matrix of the measurement equation and the state transition matrix are:

Algorithm 1 Single-Step Implementation of MMAPRIVBKF

Input: $\left\{\hat{\mathbf{x}}_{j|j}^{(j-1)}, \mathbf{P}_{j|j}^{(j-1)} \middle| k-L \le j \le k-1\right\}, \rho, \hat{y}_{k-1|k-1}, \{F_j, H_j, z_j \,|k-L \le j \le k\}$

1.Forward Kalman Filter （Forward KF）: $\left[\hat{x}_{k|k}^{(k-1)}, P_{k|k}^{(k-1)}\right] = KF\left(\hat{x}_{k|k-1}^{(k-2)}, P_{k|k-1}^{(k-2)}, F_k, \hat{Q}^{(k-1)}, \hat{R}^{(k-1)}, z_k\right)$

Backward KS: For $j = k-1:(k-L+1)$

2. $\left[\hat{x}_{j|k}^{(k-1)}, P_{j|k}^{(k-1)}\right] = KS\left(\hat{x}_{j|k}^{(k-1)}, P_{j|k}^{(k-1)}, \hat{x}_{j-1|j-1}^{(j-2)}, P_{j-1|j-1}^{(j-2)}, F_j, \hat{Q}^{(k-1)}\right)$

3. Use equations (10)-(12) to compute A_j and B_j. End loop

4. Calculate B_{K-L} using Equation (11)

$A_t = \text{median}(A_t)$， $B_t = \text{median}(B_t)$

$\hat{Q}^{(k)}$ and $\hat{R}^{(k)}$ the online estimates of

5. Calculate $\hat{y}_{k|k-1}$ $\hat{Y}_{k|k-1}$ $\hat{u}_{k|k-1}$,, and $\hat{U}_{k|k-1}$ using Equation (3)

6. Calculate $\hat{y}_{k|k}$ $\hat{Y}_{k|k}$ $\hat{u}_{k|k}$,, and $\hat{U}_{k|k}$ using Equation (8)

7. Calculate $\hat{Q}^{(k)}$ and $\hat{R}^{(k)}$

Output: $\{\hat{x}_{j|j}^{(j-1)}, P_{j|j}^{(j-1)} \,|k-L+1 \le j \le k\}, \hat{y}_{k|k}, \hat{Y}_{k|k}, \hat{u}_{k|k}, \hat{U}_{k|k}, \hat{Q}^{(k)}, \hat{R}^{(k)}$

$$\boldsymbol{F}_k = \begin{bmatrix} 1 & 0 & \Delta t & 0 \\ 0 & 0 & 1 & 0 \\ 0 & 1 & 0 & \Delta t \\ 0 & 0 & 0 & 1 \end{bmatrix} \tag{17}$$

$$\boldsymbol{H}_k = \begin{bmatrix} \dfrac{x_k}{\sqrt{x_k^{\,2} + y_k^{\,2}}} & 0 & \dfrac{y_k}{\sqrt{x_k^{\,2} + y_k^{\,2}}} & 0 \\ \dfrac{-y_k}{x_k^{\,2} + y_k^{\,2}} & 0 & \dfrac{x_k}{x_k^{\,2} + y_k^{\,2}} & 0 \end{bmatrix} \tag{18}$$

Where: $\Delta t = 15s$ is the sampling time.

The simulation target was set to move with a uniform linear velocity, an initial distance of 5000 m, and an initial azimuth of 45°. The standard deviation of the distance measurement error was set to 0.18% of the initial distance, and the standard deviation of the azimuth measurement error was set to 2°. The initial covariance matrix for the state estimation is

$$P_0 = \begin{bmatrix} 1000^2 & 0 & 0 & 0 \\ 0 & 1 & 0 & 0 \\ 0 & 0 & 1000^2 & 0 \\ 0 & 0 & 0 & 1 \end{bmatrix} \tag{19}$$

The process noise is set as

$$Q_k = \begin{bmatrix} & 0 & 0 & 0 \\ 0 & & 0 & 0 \\ 0 & 0 & & 0 \\ 0 & 0 & 0 & \end{bmatrix} \tag{20}$$

To objectively evaluate the algorithm performance, the RMSE and average root mean square error (ARMSE) were selected as core evaluation metrics, defined as follows:

$$RMSE = \sqrt{\frac{1}{N}\sum_{j=1}^{N}\left[\left(\hat{x}_k^j - x_k^j\right)^2 + \left(\hat{y}_k^j - y_k^j\right)^2\right]} \tag{21}$$

$$ARMSE_{pos} = \frac{1}{M}\sum_{k=1}^{M}\sqrt{\frac{1}{N}\sum_{j=1}^{N}\left[\left(\hat{x}_k^j - x_k^j\right)^2 + \left(\hat{y}_k^j - y_k^j\right)^2\right]} \tag{22}$$

Where N represents the total number of Monte Carlo simulations, M denotes the total number of time steps in a single simulation, x_k^j and $\hat{x}_k^j$ correspond to the true and estimated values at time step k in the `i`th simulation. The calculation formulas for RMSE and ARMSE in terms of heading and velocity are identical to Equations (21) and (22) respectively.

3.2 Single-Run Performance

To validate the performance advantages of the proposed algorithm for state estimation tasks, a uniform linear motion simulation scenario was established for comparative experiments. The experiment focused on a typical uniform linear motion target with parameters set as described in Section 4 of this paper. Under a discrete-time sequence, 100 consecutive observation data points were collected to simulate the continuous monitoring process of moving targets in practical engineering applications. The EKF and NAPRIVBKF were selected as comparison algorithms. Comparative experiments were conducted under identical initial parameters and observation conditions. Initial parameters are: $L = 5$， $\rho = 1 - \exp(-4)$， $\hat{u}_{0|0} = \hat{y}_{0|0} = 0$， $\mathbf{Y}_{0|0} = \mathbf{0}_4$， $\mathbf{U}_{0|0} = \mathbf{0}_2$。

The results of the single-run simulation are shown in Figure 1.

Evaluations based on the single-run simulation confirm the state estimation accuracy of the proposed algorithm. In terms of RMSE for range, bearing, and velocity, the proposed method exhibits superior performance in position estimation bias and velocity tracking stability during uniform motion compared to benchmarks. The overall estimation results showed a higher degree of fit with the actual motion trajectory of the

target, significantly outperforming the accuracy loss caused by the linearization errors in the nonlinear approximation process of the EKF. It also overcomes the limitation of NAPRIVBKF of "averaging" the estimation of noise characteristics within the window, fully demonstrating its state estimation performance advantages in scenarios of uniform linear motion.

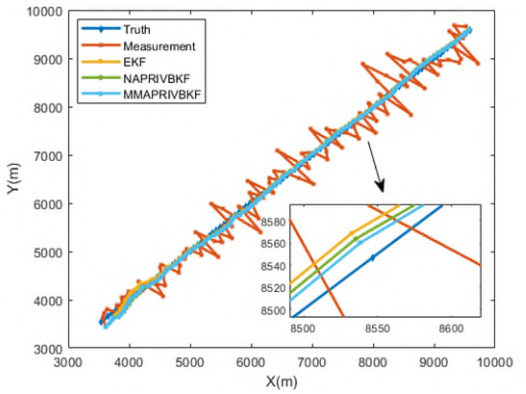


Fig.1 Single-run simulation results

3.3 Algorithm Performance Analysis

To further quantify the superiority of the proposed algorithm in state estimation accuracy, a RMSE comparison experiment was designed for three key metrics—distance, bearing, and velocity—under uniform linear motion scenarios. This provides an intuitive assessment of the estimation accuracy of the algorithm for the spatial position, direction, and angle of the target. The simulations were conducted using 500 Monte Carlo iterations.

As shown in Figures 2-4, the three RMSE metrics of the proposed algorithm demonstrated significant advantages in the later stages. This stems from the algorithm design, which combines a slide window median mechanism with variational Bayesian noise adaptive estimation. For distance estimation, the insufficient accumulation of effective observation data within the slide window during the first 50 observation points prevents the adaptive learning of the noise covariance matrix from fully converging, resulting in a slightly higher distance estimation bias during the initial phase. After the number of observations increased to 50, the data sample size within the window sufficiently supported the accurate inference of the statistical characteristics of the noise. Concurrently, the median mechanism progressively suppresses anomalous observations, leading to a significant reduction and stabilization of the distance RMSE.

In contrast, heading and velocity estimation demonstrated clear advantages after only 20 observations. This is because these state variables exhibit lower sensitivity to noise variations than distance: heading relies on the relative trend of angular observations, whereas velocity leverages the continuity characteristic of uniform motion. Both can achieve preliminary adaptation to the noise covariance with limited effective data within the window. Combined with the analytical updates of the variational Bayesian method to the noise posterior distribution, this rapidly mitigates the effects of the EKF linearization errors and NAPRIVBKF noise adaptation lag, enabling an earlier demonstration of the estimation accuracy advantages.

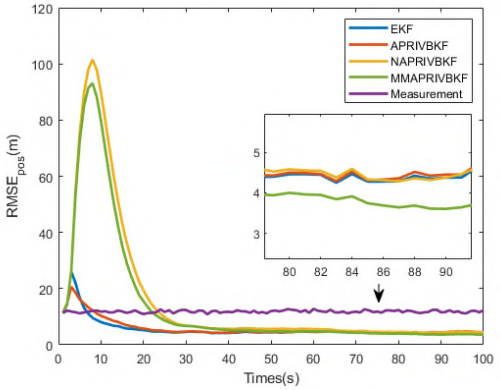


Fig.2 Distance RMSE Comparison

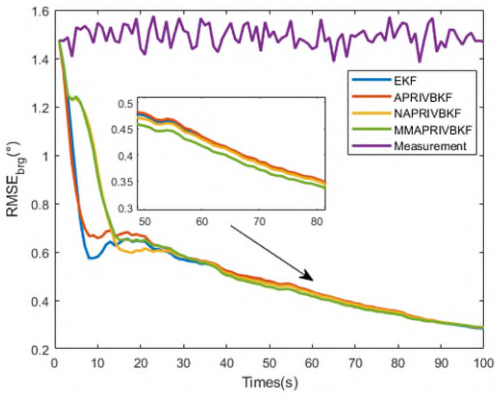


Fig3. Azimuth RMSE Comparison

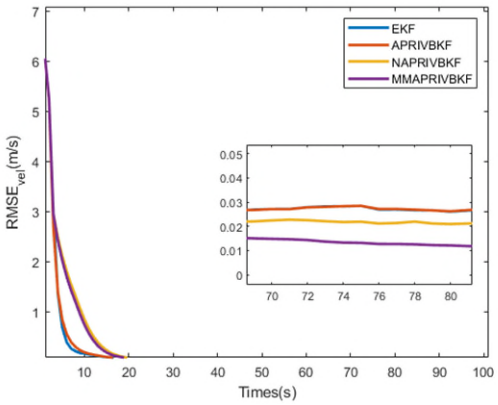


Fig4. Velocity RMSE Comparison

To validate the impact of the slide window size on the algorithm performance, a comparative experiment with variable window lengths was designed, and NAPRIVBKF was selected as the baseline algorithm. While maintaining consistent experimental parameters, the slide window length of the proposed algorithm was set to [1, 2, 4, 6, 8, 10, 12, 14, 16, 18, 20]. By calculating the mean RMSE for the range, bearing, and velocity under different window configurations, we systematically analyzed the impact of window size variations on the estimation accuracy of both algorithms. This validated the adaptability and superiority of the proposed algorithm in scenarios requiring dynamic window parameter adjustment.

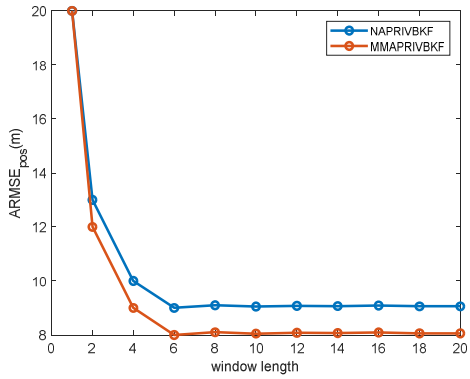


Fig. 5. Effect of Window Size on Range ARMSE

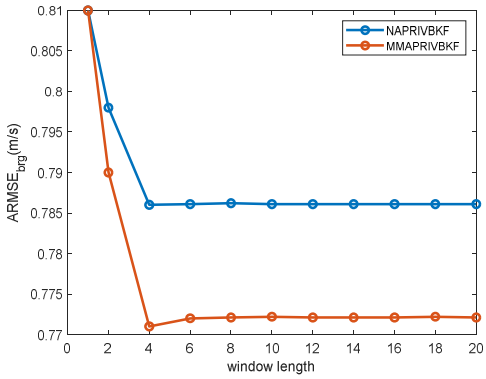


Fig6. Effect of Window Size on Azimuth ARMSE

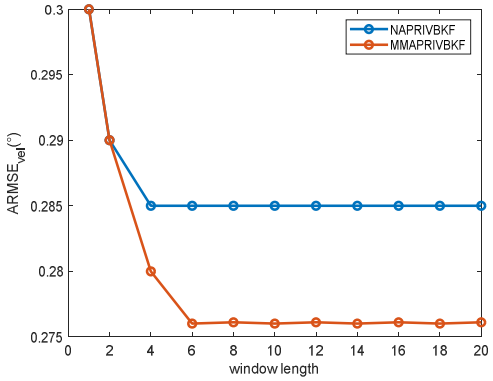


Fig. 7. Effect of Window Size on Velocity ARMSE

The experimental results demonstrate that regardless of the slide window size setting, the proposed method consistently outperforms NAPRIVBKF in the ARMSE metrics for all three core states: distance, bearing, and velocity. As the window size gradually increased from 1 to 4, the ARMSE for the distance, bearing, and velocity progressively decreased. When the window size exceeded 4, the ARMSE stabilized, and further increases in the window size no longer affected the algorithm's performance. A window size of 5 was selected to ensure real-time capability.

To validate the robustness of the algorithm under varying noise interference intensities, comparative experiments with different error levels were designed. Using uniform linear motion as the baseline scenario, simulation experiments were conducted by adjusting the error coefficients. The six sets of measurement errors with varying degrees are listed in Table 1.

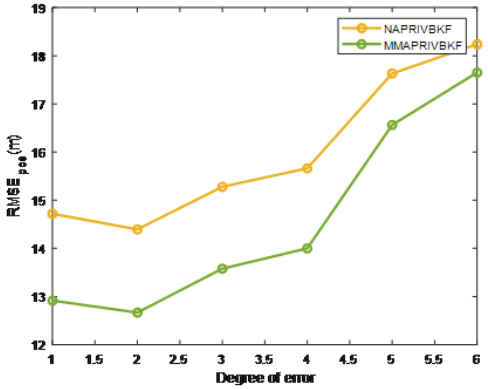


Fig. 8. Comparison of AMRSE at Different Error Levels

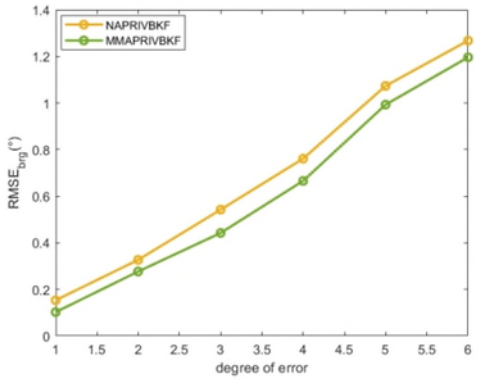


Fig9. Comparison of AMRSE at Different Error Levels

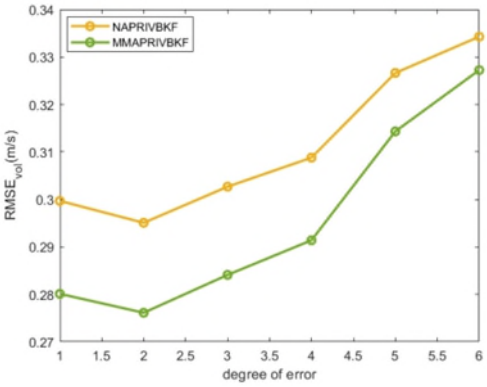


Fig. 10. Comparison of AMRSE at Different Error Levels

From the experimental results shown in Figs. 8-10, both algorithms exhibit an upward trend in the ARMSE as the error severity increases. However, the performance advantage of the proposed algorithm becomes more pronounced as the error intensity rises. At the highest error level

Table 1 Six Sets of Measurement Error Settings

	1	2	3	4	5	6
pos(m)	x*0.01	x*0.012	x*0.014	x*0.016	x*0.018	x*0.02
brg(°)	0.5	1	1.5	2	2.5	3

in the experiments, the proposed method achieved ARMSE reductions of 8.52%, 24.12%, and 7.19% compared to the SWAKF for distance, bearing, and velocity, respectively, highlighting its superior capability in handling high uncertainty. These results underscore the effectiveness and reliability of the proposed algorithm compared to the other algorithms under large measurement errors.

4 Summary

To address the challenge of balancing estimation efficiency and computational complexity in the real-time applications of traditional slide window variational adaptive Kalman filters, this study proposes an improved adaptive Kalman filter algorithm that incorporates a slide median window. Building upon the strengths of the variational Bayesian framework, this method achieves dual optimization: First, by approximating the smoothed posterior distribution of the state vector within the slide window, the posterior distribution of the noise covariance matrix is analytically updated to an inverse Wishart distribution. This eliminates the fixed-point iteration process in traditional approaches, significantly enhancing computational efficiency. Second, it innovatively introduces a slide median window mechanism. This mechanism preserves the adaptive learning capability for unknown target states and measurement noise covariance matrices while effectively suppressing occasional extreme errors, thereby reducing the impact of random disturbances on the final filtering results. Simulation results demonstrate that compared to the original SWVAKF method, the proposed approach achieves further reductions in RMSE for range, bearing, and velocity. This provides a solution for state estimation in complex noise environments that holds both theoretical value and engineering significance.

Declarations

Conflict of interest The authors declare that they have no conflict of interest.

Funding ： Not applicable

Acknowledgments

This work was supported by the Innovation Project of Colleges and Universities in Shanxi Province [Grant No. 2023L503].

References

[1] Khodarahmi M, Maihami V. A review on Kalman filter models[J]. Archives of Computational Methods in Engineering, 2023, 30(1): 727-747

[2] Wang B, Sun Z, Jiang X, et al. Kalman filter and its application in data assimilation[J]. Atmosphere, 2023, 14(8): 1319

[3] Li Q, Li R, Ji K, et al. Kalman filter and its application[C]//2015 8th international conference on intelligent networks and intelligent systems (ICINIS). IEEE, 2015: 74-77

[4] Hesar H D, Hesar A D. Adaptive dual augmented extended Kalman filtering of ECG signals[J]. Measurement, 2025, 239: 115457

[5] X. Gao, D. You and S. Katayama, "Seam tracking monitoring based on adaptive Kalman filter embedded elman neural network during highpower fiber laser welding," IEEE Trans. Ind. Electron, vol. 59, no. 11, pp. 4315−4325, Nov. 2012

[6] Wang B, Sun Z, Jiang X, et al. Kalman filter and its application in data assimilation[J]. Atmosphere, 2023, 14(8): 1319

[7] Bai Y, Yan B, Zhou C, et al. State of art on state estimation: Kalman filter driven by machine learning[J]. Annual Reviews in Control, 2023, 56: 100909

[8] Lan C, Guo R, Yang J, et al. Adaptive backward-correction extended Kalman filter for small amounts of measurement data[J]. Ocean Engineering, 2025, 341: 122500

[9] Ullah I, Su X, Zhu J, et al. Evaluation of Localization by Extended Kalman Filter, Unscented Kalman Filter, and Particle Filter-Based Techniques[J]. Wireless Communications and Mobile Computing, 2020, 2020(1): 8898672

[10] Wan E A, Van Der Merwe R. The unscented Kalman filter for nonlinear estimation[C]//Proceedings of the IEEE 2000 adaptive systems for signal processing, communications, and control symposium (Cat. No. 00EX373). Ieee, 2000: 153-158

[11] Lan H, Hu J, Wang Z, et al. Variational nonlinear Kalman filtering with unknown process noise covariance[J]. IEEE Transactions on Aerospace and Electronic Systems, 2023, 59(6): 9177-9190

[12] Greenbaum A. Estimating the attainable accuracy of recursively computed residual methods[J]. SIAM journal on matrix analysis and applications, 1997, 18(3): 535-551

[13] Lupu C, Borne P, Popescu D. Multi-model adaptive control systems[J]. Journal of Control Engineering and Applied Informatics, 2008, 10(1): 49-56

[14] Yang X, Mu Y, Cao K, et al. Robust kernel recursive adaptive filtering algorithms based on M-estimate[J]. Signal Processing, 2023, 207: 108952

[15] Zhu T, Wang S, Fan Y, et al. Improved forgetting factor recursive least square and adaptive square root unscented Kalman filtering methods for online model parameter

identification and joint estimation of state of charge and state of energy of lithium-ion batteries[J]. Ionics, 2023, 29(12): 5295-5314

[16] Cheng Y, Zhang S, Wang X, et al. Self-tuning process noise in variational bayesian adaptive kalman filter for target tracking[J]. Electronics, 2023, 12(18): 3887

[17] Wang B, Huang Y, Luo L, et al. An improved adaptive Kalman filter for in-motion initial alignment of GPS-aided sins[C]//International Conference on Autonomous Unmanned Systems. Singapore: Springer Singapore, 2021: 1462-1472

[18] Huang Y, Zhu F, Jia G, et al. A slide window variational adaptive Kalman filter[J]. IEEE Transactions on Circuits and Systems II: Express Briefs, 2020, 67(12): 3552-3556

[19] Y. Huang, Y. Zhang, N. Li, Z. Wu, and J. Chambers, ″A novel robust Student′ s t-based Kalman filter,″ IEEE Trans. Aerosp. Electron. Syst., vol. 53, no. 3, pp. 1545−1554, Jun. 2017

[20] A. O′ Hagan, and J. J. Forster, Kendall′ s Advanced Theory of Statistics: Bayesian Inference., London, U.K.: Arnold, 2004

[21] Duník J, Straka O, Kost O, et al. Noise covariance matrices in state‐space models: A survey and comparison of estimation methods—Part I[J]. International Journal of Adaptive Control and Signal Processing, 2017, 31(11): 1505-1543

[22] Hartikainen S S J. Variational Bayesian adaptation of noise covariances in non-linear Kalman filtering[J]. arXiv preprint arXiv:1302.0681, 2013.

[23] C. M. Bishop, Pattern Recognition and Machine Learning (Information Science and Statistics). Springer-Verlag New York, 2006

[24] D. Tzikas, A. Likas, and N. Galatsanos, “The variational approximation for Bayesian inference,” IEEE Signal Processs Mag., vol. 25, no. 6, pp. 131–146, Nov. 2008)

[25] Y. Huang, Y. Zhang, Z. Wu, N. Li, and J. Chambers, “A novel adaptive Kalman filter with inaccurate process and measurement noise covariance matrices,” IEEE Trans. Automat. Control, vol. 63, no. 2, pp. 594–601, Feb. 2018

[26] Y. Huang, Y. Zhang, N. Li, and J. Chambers, “A robust Gaussian approximate fixed-interval smoother for nonlinear systems with heavytailed process and measurement noises,” IEEE Signal Process. Lett., vol. 23, no. 4, pp. 468–472, Apr. 2016.

[27] Qiao S, Fan Y, Wang G, et al. Modified strong tracking slide window variational adaptive Kalman filter with unknown noise statistics[J]. IEEE Transactions on Industrial Informatics, 2022, 19(8): 8679-8690

[28] Qiao S, Fan Y, Wang G, et al. Strong tracking square-root modified sliding-window variational adaptive Kalman filtering with unknown noise covariance matrices[J]. Signal Processing, 2023, 204: 108837

[29] Fujii K. Extended kalman filter[J]. Refernce Manual, 2013, 14: 41